University Library

MINERVA ACCESS

A gateway to Melbourne's research publications

Minerva Access is the Institutional Repository of The University of Melbourne

Author/s:
Sett, A;Foo, GWC;Kenna, KR;Sutton, RJ;Perkins, EJ;Sourial, M;Rogerson, SR;Manley, BJ;Davis, PG;Pereira-Fantini, PM;Tingay, DG

Title:
Quantitative lung ultrasound detects dynamic changes in lung recruitment in the preterm lamb

Date:
2023-05-01

Citation:
Sett, A., Foo, G. W. C., Kenna, K. R., Sutton, R. J., Perkins, E. J., Sourial, M., Rogerson, S. R., Manley, B. J., Davis, P. G., Pereira-Fantini, P. M. & Tingay, D. G. (2023). Quantitative lung ultrasound detects dynamic changes in lung recruitment in the preterm lamb. Pediatric Research, 93 (6), pp.1591-1598. https://doi.org/10.1038/s41390-022-02316-0.

Persistent Link:
https://hdl.handle.net/11343/320108

License:
CC BY

European Society for Paediatric Research
Society for Pediatric Research
www.nature.com/pr

BASIC SCIENCE ARTICLE OPEN

Check for updates

Quantitative lung ultrasound detects dynamic changes in lung recruitment in the preterm lamb

Arun Sett[1,2,3,4,5]✉, Gillian W. C. Foo[2], Kelly R. Kenna[1], Rebecca J. Sutton[1,6], Elizabeth J. Perkins[1], Magdy Sourial[6], Sheryle R. Rogerson[2,4,5], Brett J. Manley[1,2,4], Peter G. Davis[1,2,4], Prue M. Pereira-Fantini[1,2,7] and David G. Tingay[1,2,7,8]

© Crown 2022

BACKGROUND: Lung ultrasound (LUS) may not detect small, dynamic changes in lung volume. Mean greyscale measurement using computer-assisted image analysis (Q-LUS$_{MGV}$) may improve the precision of these measurements.
METHODS: Preterm lambs ($n = 40$) underwent LUS of the dependent or non-dependent lung during static pressure–volume curve mapping. Total and regional lung volumes were determined using the super-syringe technique and electrical impedance tomography. Q-LUS$_{MGV}$ and gold standard measurements of lung volume were compared in 520 images.
RESULTS: Dependent Q-LUS$_{MGV}$ moderately correlated with total lung volume (rho = 0.60, 95% CI 0.51–0.67) and fairly with right whole (rho = 0.39, 0.27–0.49), central (rho = 0.38, 0.27–0.48), ventral (rho = 0.41, 0.31–0.51) and dorsal regional lung volumes (rho = 0.32, 0.21–0.43). Non-dependent Q-LUS$_{MGV}$ moderately correlated with total lung volume (rho = 0.57, 0.48–0.65) and fairly with right whole (rho = 0.43, 0.32–0.52), central (rho = 0.46, 0.35–0.55), ventral (rho = 0.36, 0.25–0.47) and dorsal lung volumes (rho = 0.36, 0.25–0.47). All correlation coefficients were statistically significant. Distinct inflation and deflation limbs, and sonographic pulmonary hysteresis occurred in 95% of lambs. The greatest changes in Q-LUS$_{MGV}$ occurred at the opening and closing pressures.
CONCLUSION: Q-LUS$_{MGV}$ detected changes in total and regional lung volume and offers objective quantification of LUS images, and may improve bedside discrimination of real-time changes in lung volume.

Pediatric Research; https://doi.org/10.1038/s41390-022-02316-0

IMPACT:

- Lung ultrasound (LUS) offers continuous, radiation-free imaging that may play a role in assessing lung recruitment but may not detect small changes in lung volume.
- Mean greyscale image analysis using computer-assisted quantitative LUS (Q-LUS$_{MGV}$) moderately correlated with changes in total and regional lung volume.
- Q-LUS$_{MGV}$ identified opening and closing pressure and pulmonary hysteresis in 95% of lambs.
- Computer-assisted image analysis may enhance LUS estimation of lung recruitment at the bedside.
- Future research should focus on improving precision prior to clinical translation.

INTRODUCTION

Continuous imaging of lung recruitment in neonatal patients is an attractive alternative to indirect physiological estimators of lung volume, such as peripheral oxygen saturations and ventilation parameters, or conventional radiography.[1,2] For this purpose, lung ultrasound (LUS) and electrical impedance tomography (EIT) are promising point of care, radiation-free imaging modalities.[3] Ultrasound interaction with the pleura produces consistent artefact patterns that correspond with lung aeration,[4] forming the foundations of visual scoring systems for LUS.[5,6] Despite traditional LUS scoring systems reliably diagnosing some neonatal respiratory conditions,[5,7–9] and detecting large lung volume changes in adults[10] and in animal models of the preterm lung,[11] they cannot measure small changes in lung volume.[12] There are few reports of the accuracy of LUS against gold-standards measurements of lung volume such as gas washout, computed tomography (CT) or the super-syringe technique,[13] and only one has specifically studied the preterm lung.[11] Thus, whilst a role for LUS is established, some aspects such as the assessment of preterm lung recruitment need further evaluation.[14–16]

The shortcomings of traditional LUS may be overcome by supplementing interpretation with computer-assisted image

[1]Neonatal Research, Murdoch Children's Research Institute, Parkville, VIC, Australia. [2]Newborn Research Centre, The Royal Women's Hospital, Parkville, VIC, Australia. [3]Joan Kirner Women's and Children's Hospital, Western Health, St Albans, VIC, Australia. [4]Department of Obstetrics and Gynaecology, The University of Melbourne, Parkville, VIC, Australia. [5]Paediatric Infant Perinatal Emergency Retrieval, The Royal Children's Hospital, Parkville, VIC, Australia. [6]Translational Research Unit, Murdoch Children's Research Institute, Parkville, VIC, Australia. [7]Department of Paediatrics, The University of Melbourne, Parkville, VIC, Australia. [8]Department of Neonatology, The Royal Children's Hospital, Parkville, VIC, Australia. ✉email: arun.sett@mcri.edu.au

Received: 11 July 2022 Revised: 24 August 2022 Accepted: 7 September 2022
Published online: 27 September 2022

analysis. Measurement of the average greyness of a whole or specific region of an image is a simple form of image analysis. Quantitative lung ultrasound with analysis of the mean greyscale value (Q-LUS$_{MGV}$) measures the greyness of each pixel within a defined region of interest (ROI) and calculates a numerical mean grey value for the ROI. Though the human perception of greyscale colours is limited,[17] Q-LUS$_{MGV}$ is capable of resolving the full breadth of the greyscale spectrum,[13,18] making it suitable for discriminating small changes in lung volume in real-time.

EIT measures the real-time change in lung volume by analysing changes in electrical bioimpedance associated with varying lung aeration.[3] EIT has an established role in critical care research, and reliably maps the pressure–volume (PV) relationship of the preterm lung in humans and animals.[19–21] As EIT measurement of lung recruitment has been validated against CT,[22,23] it serves as an appropriate comparator for LUS validation studies.

We hypothesised that Q-LUS$_{MGV}$ would detect real-time changes in lung volume, demonstrate pulmonary hysteresis and identify the opening and closing pressure of the lung. To explore this, we compared Q-LUS$_{MGV}$ of the pleural region of LUS images acquired from preterm lambs during mapping of the PV relationship of the respiratory system to global and regional lung volumes measured by the super-syringe method[21] and EIT respectively.

METHODS

This study was part of a larger programme investigating the role of different respiratory strategies in the initiation of preterm lung injury at birth. The study was approved by the Murdoch Children's Research Institute Animal Ethics Committee, Melbourne, Australia in accordance with National Health and Medical Research Council (Australia) guidelines and is reported as per the ARRIVE guidelines.[24]

Animal preparation

Preterm lambs of 124–128 days gestation (term gestation 143–145 days) were delivered from anaesthetised, betamethasone exposed, Border-Leicester/Merino ewes via caesarian section. Following exteriorisation for carotid vessel instrumentation, intubation proceeded with a 4.0 mm cuffed endotracheal tube (ETT) followed by passive lung liquid drainage. As part of the protocol of the primary study, after 15 min of mechanical ventilation, lambs were maintained on placental support for 30 min whilst apnoeic with the ETT clamped. Next, the ETT was unclamped and opened to the atmosphere for 2 min whilst lambs were apnoeic and the static PV relationship of the respiratory system was mapped using a calibrated glass syringe as previously described.[21] Lungs were inflated and then deflated using pre-defined pressure increments between atmospheric (0 centimetres of water [cm H_2O]) and maximal inflation pressure (35 cm H_2O). At completion, the umbilical cord was clamped and a lethal dose of sodium pentobarbitone (100 mg/kg) was administered.

Lung ultrasound (LUS)

LUS was performed using a Logiq E (GE Healthcare, Wauwatosa, WI) and Terason USMART 3200T (Terason, Burlington, MA) ultrasound system with a 12-megahertz broadband linear transducer. Gain was set to 50 decibels, depth to 2.5 cm and the focal zone was positioned at the pleural line. Filters were deactivated. Details on ultrasound settings and techniques are described in the Supplementary methods. All animals were imaged in the supine position. Ultrasound images were acquired from the right lower lateral (dependent) and right anterior upper (non-dependent) thorax at each pressure increment during the inflation and deflation series. These correspond to the central and ventral EIT regions respectively. Sonographic opening and closing pressure were defined as the pressure increment preceding the largest change in Q-LUS$_{MGV}$. Sonographic hysteresis was defined as the presence of distinct inflation and deflation limbs on PV curves constructed from Q-LUS$_{MGV}$, with on average higher measurements on the deflation limb when compared to the corresponding inflation pressures.

Computer-assisted greyscale analysis

Uncompressed LUS images taken at each pressure increment were de-identified and imported into FIJI, ImageJ (National Institute of Health, Bethesda, Maryland).[25] Representative still images were selected and analysed in 8-bit format for measurement of Q-LUS$_{MGV}$ of the pleural ROI. Two investigators (A.S., 4-year LUS experience and G.F. 1-year LUS experience) manually delineated the pleural ROI (Fig. 1) on anonymized images in random order. Q-LUS$_{MGV}$ was determined by measuring the sum grey value of all the pixels within the ROI and dividing the result by the total number of pixels within the ROI[25] using the built-in measurement package. In 8-bit pixel depth, Q-LUS$_{MGV}$ ranges from 0 (black) to 255 (white). Q-LUS$_{MGV}$ is measured in arbitrary units.

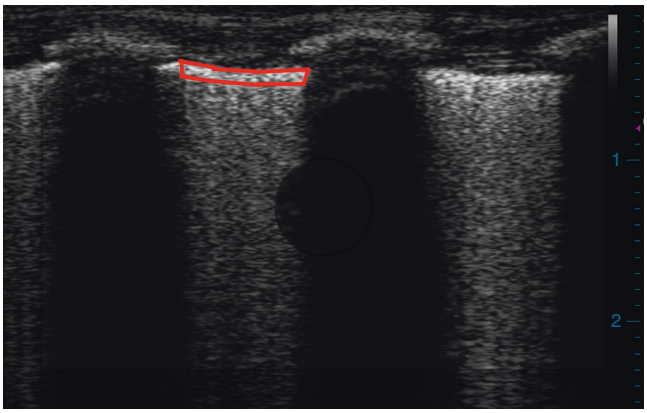


Fig. 1 ROI (red tracing) for measurement of Q-LUS$_{MGV}$. The ROI was delineated by (1) superior margin defined by the pleural surface; (2) lateral margin defined by the rib shadows; and (3) inferior margin defined by a depth of 50 pixels corresponding to one millimetre in depth. Q-LUS$_{MGV}$; quantitative lung ultrasound mean grey value.

Electrical impedance tomography

Continuous EIT (Pioneer system, Sentec AG, Landquart, Switzerland) assessment of lung volumes was made at 48 frames/s from before commencing ventilation to study completion, including the mapping of the PV relationship, using our previously reported methodology.[21] Data were reconstructed using an anatomically correct finite element model of the lamb thorax filtered to the respiratory domain.[3,20] The time-course EIT signal for the whole lung was calibrated against the volume changes measured by the super syringe,[21] and the lung volumes of the right whole, dorsal, central and ventral lung were determined from weighting the EIT pixel distribution of each region to the calibrated whole lung volumes.[26,27]

Statistical analysis

As this study was part of a larger research programme, a convenience sample of 40 lambs was chosen. Baseline characteristics were reported as mean and standard deviation. Q-LUS$_{MGV}$ and lung volumes were reported as median and interquartile range (IQR). Change in Q-LUS$_{MGV}$ was defined as the increase in value relative to that measured at 0 cm H_2O. Correlation was calculated using Spearman's correlation coefficient (rho) as Q-LUS$_{MGV}$ distribution was skewed. A strong correlation was defined as rho ≥0.70, moderate ≥0.50, fair ≥0.30 and weak <0.30. Friedman's test and a post hoc Wilcoxon signed rank sum test with a Bonferroni correction for multiple comparisons was used to compare Q-LUS$_{MGV}$ between each pressure increment. The pooled Q-LUS$_{MGV}$ of the inflation and deflation series were fitted to the sigmoidal model of the PV relationship proposed by Venegas et al.[28] using least-squares non-linear regression. The predicted opening and closing pressures were then calculated from the model by differentiating the regression equation using the best-fit parameters and finding peaks in the differential curve. This corresponded to the maximum rate of change in both Q-LUS$_{MGV}$ and EIT curves. Interobserver variability was calculated using an intraclass correlation coefficient with a two-way random effects model. Significance was set at <0.05. Analysis was performed using GraphPad Prism (V9.1.2, GraphPad Software, San Diego) and R (R: A Language and Environment for Statistical Computing, Vienna, Austria, 2021).[29]

RESULTS

Forty lambs were studied (62% male). In our cohort, no pneumothoraces occurred during ventilation or mapping of PV

relationship and no lambs had foetal distress or acidosis. A total of 520 LUS images were acquired (260 dependent and 260 non-dependent). Characteristics of the lambs are shown in Table 1.

Figures 2 and 3 show measured lung volumes at each pressure increment during mapping of the PV relationship (grey dashed line). The median (IQR) lung volume at 35 cm H_2O was 24 (19–28) ml/kg (of body weight) and 22 (17–25) ml/kg in the dependent and non-dependent imaging groups, respectively. Hysteresis was evident in all lambs (individual PV relationships, Supplementary Figs. E1 and E2). Opening and closing pressures were 20 cm H_2O and 10 cm H_2O respectively in 19 out of 20 lambs in the dependent group and 18 out of 20 lambs in the non-dependent group. This corresponded to median (IQR) lung volumes of 6.5 (6–8) ml/kg and 12 (10–15.5) ml/kg in the dependent group and 5.5 (4.5–6.5) ml/kg and 10 (7.5–12) ml/kg in the non-dependent group.

Total lung volume derived from the super-syringe method

Dependent LUS. Q-LUS_{MGV} of the dependent lung moderately correlated with changes in total lung volume (rho = 0.60, $p < 0.0001$, CI 0.51–0.67, Fig. 2). Q-LUS_{MGV} was able to differentiate between pressures (median volume [IQR]) of 15 cm H_2O (5 [4–5] ml/kg) and 30 cm H_2O (18 [15–22] ml/kg) during the inflation series ($p = 0.01$), and 20 cm H_2O (19 [15–23] ml//kg) and 10 cm H_2O (12 [10–16] ml/kg) during the deflation series ($p = 0.04$) (Supplementary Table E1). Q-LUS_{MGV} demonstrated distinct inflation and deflation limbs, and pulmonary hysteresis in all lambs (Individual pressure/Q-LUS_{MGV} relationships, Supplementary Fig. E3a, b).

Non-dependent LUS. Q-LUS_{MGV} of the non-dependent lung moderately correlated with changes in total lung volume (rho = 0.57, $p < 0.0001$, CI 0.48–0.65, Fig. 3). Q-LUS_{MGV} was able to differentiate between pressures (median volume [IQR]) of 20 cm H_2O (5 [4–7] ml/kg) and 30 cm H_2O (16 [12–20] ml/kg) during the inflation series ($p = 0.01$), and 10 cm H_2O (10 [8–12] ml//kg) and 5 cm H_2O (5 [4–7] ml/kg) during the deflation series ($p = 0.01$) (Supplementary Table E2). Q-LUS_{MGV} demonstrated distinct inflation and deflation limbs, and pulmonary hysteresis in 18/20 lambs (individual pressure/Q-LUS_{MGV} relationships, Supplementary Fig. E4a, b).

Table 1. Lamb characteristics ($n = 40$).

Mean (SD) gestational age, days	125 (1)	
Male, *n* (%)	25 (62)	
Singleton, *n* (%)	12 (30)	
Mean (SD) birth weight, g	3002 (450)	
Arterial blood gas analysis, mean (SD)	Cord	15 min
pH	7.36 (0.05)	7.40 (0.06)
pCO_2 (mm Hg)	44 (4)	36 (4)
Base excess (mmol/l)	−0.6 (2.9)	−2.0 (3.2)

pCO_2 partial pressure of carbon dioxide, *SD* standard deviation.

Regional lung volume derived from EIT

Dependent LUS. Q-LUS_{MGV} of the dependent lung correlated fairly with changes in regional volume (Fig. 4) of the right whole lung (rho = 0.39, $p < 0.0001$, CI 0.27–0.49), and central (rho = 0.38, $p < 0.0001$, CI 0.27–0.48), ventral (rho = 0.41, $p < 0.0001$, CI 0.31–0.51) and dorsal regions (rho = 0.32, $p < 0.0001$, CI 0.21–0.43).

Non-dependent LUS. Q-LUS_{MGV} of the non-dependent lung fairly correlated with changes in regional volume (Fig. 5) of the right whole lung (rho = 0.43, $p < 0.001$, CI 0.32–0.52), and central (rho = 0.46, $p < 0.0001$, CI 0.35–0.55), ventral (rho = 0.36, $p < 0.0001$, CI 0.25–0.47) and dorsal regions (rho = 0.36, $p < 0.0001$, CI 0.25–0.47).

Interobserver agreement

There was excellent agreement between both investigators for the dependent (ICC = 0.87, 95% CI 0.83–0.90, Supplementary Fig. E5) and non-dependent lung Q-LUS_{MGV} (ICC = 0.93, 0.92–0.95, Supplementary Fig. E6).

Modelling the pressure–volume relationships

The sigmoidal model of the PV relationship proposed by Venegas et al.[28] was able to be fitted to the pooled inflation (adjusted $R^2 = 0.90$, runs test; $p = 0.80$) and deflation series (adjusted $R^2 = 0.93$, runs test; $p = 0.54$) derived from the Q-LUS_{MGV} of the dependent region (Supplementary Fig. E7), and from the pooled inflation (adjusted $R^2 = 0.98$, runs test; $p = 0.97$) and deflation series (adjusted $R^2 = 0.92$, runs test; $p > 0.99$) derived from the Q-LUS_{MGV} of the non-dependent region (Supplementary Fig. E8). Similarly, the model was able to be fitted to the pooled inflation (adjusted $R^2 = 0.99$, runs test; $p = 0.2$) and deflation series (adjusted $R^2 = 0.99$, runs test; $p = 0.52$) derived from EIT of the dependent region (Supplementary Fig. E9), and from the pooled inflation (adjusted $R^2 = 0.97$, runs test; $p = 0.54$) and deflation series (adjusted $R^2 = 0.98$, runs test; $p = 0.33$) derived from EIT of the non-dependent region (Supplementary Fig. E10). The predicted opening and closing pressures from both Q-LUS_{MGV} and EIT

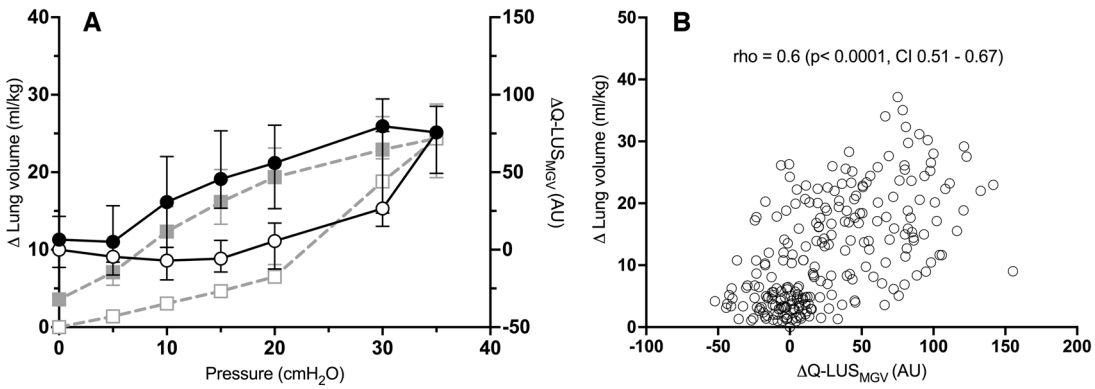


Fig. 2 Dependent lung imaging. A Static PV curve derived from the super-syringe method (squares, grey dashed line) and ΔQ-LUS_{MGV} (circles, solid black line). All data are represented as median (IQR). ΔQ-LUS_{MGV} is normalised to baseline. Open shapes represent the inflation limb and closed shapes the deflation limb. **B** Correlation between ΔQ-LUS_{MGV} and total lung volume. AU arbitrary units, CI confidence interval, cm H_2O centimetres of water, ml/kg, rho Spearman's correlation coefficient, Q-LUS_{MGV} quantitative lung ultrasound mean grey value. Left axis: lung volume (ml/kg). Right axis: ΔQ-LUS_{MGV}.

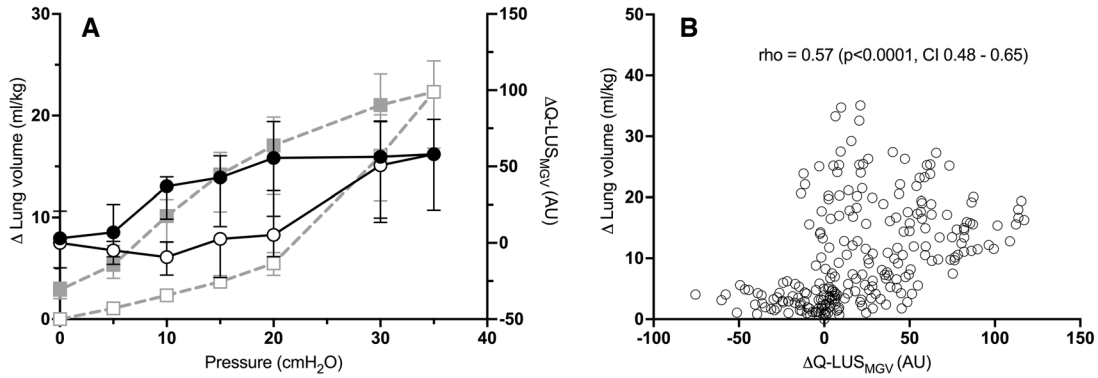


Fig. 3 Non-dependent lung imaging. A Static PV curve derived from the super-syringe method (squares, grey dashed line) and ΔQ-LUS$_{MGV}$ (circles, solid black line). All data are represented as median (IQR). ΔQ-LUS$_{MGV}$ normalised to baseline. Open shapes represent the inflation limb and closed shapes the deflation limb. **B** Correlation between ΔQ-LUS$_{MGV}$ and total lung volume. AU arbitrary units, CI confidence interval, cm H_2O centimetres of water, ml/kg, rho Spearman's correlation co-efficient, Q-LUS$_{MGV}$ quantitative lung ultrasound mean grey value. Left axis: lung volume (ml/kg). Right axis: ΔQ-LUS$_{MGV}$.

of the dependent lung (opening pressure; 25 cm H_2O in both, closing pressure; 15 vs 12 cm H_2O respectively, Supplementary Figs. E11 and E12) and the non-dependent lung (opening pressure; 25 cm H_2O in both, closing pressure; 12 vs 15 cm H_2O respectively, Supplementary Figs. E13 and E14) were similar.

DISCUSSION

As chest x-ray is a poor indicator of lung volume in preterm infants,[2] neonatal clinicians are reliant on physiological approximations to guide lung recruitment.[30–32] LUS may assist in guiding lung recruitment, but current LUS scoring systems poorly differentiate small changes in lung volume.[12] In this experiment we evaluated the ability of mean greyscale analysis using computer-assisted quantitative lung ultrasound (Q-LUS$_{MGV}$) to measure changes in lung volume. Q-LUS$_{MGV}$ moderately correlated with changes in total and regional lung volume in preterm lambs and was able to detect the opening and closing pressures of the respiratory system, and pulmonary hysteresis in 38 of 40 animals. In addition, Q-LUS$_{MGV}$ was able to detect relatively small changes in total lung volume during the deflation series. Finally, PV curves constructed from Q-LUS$_{MGV}$ measurements demonstrated distinct inflation and deflation limbs that were able to be fitted to a known mathematical model of the PV relationship. Our findings suggest that Q-LUS$_{MGV}$ detects key features of the PV relationship and may enhance the capability of LUS to monitor real-time changes in lung volume.

Quantitative ultrasound is an emerging field. Corradi et al. compared the accuracy of greyscale analysis to chest radiography, traditional LUS and CT diagnosis of pneumonia in adults.[33] When compared to CT as a gold standard, quantitative LUS outperformed both chest radiography and traditional LUS in diagnosing pneumonia and significantly correlated with CT-detected non-aerated lung. The same authors demonstrated that when compared to pulmonary capillary wedge pressure and transpulmonary thermodilution, quantitative LUS outperformed traditional LUS in detecting pulmonary oedema in ventilated adults.[34] Compared with previous studies comparing chest radiography to gold standard measurements of lung volume,[2] Q-LUS$_{MGV}$ exhibited a higher correlation with absolute measures of lung volume. This improved performance may be due to the dynamic nature of ultrasound imaging and the ability of Q-LUS$_{MGV}$ to detect small changes in lung volumes that are not detected using other modalities. These findings suggest that Q-LUS$_{MGV}$ supplementation may refine LUS detection of dynamic change lung volume, and subsequently guide lung recruitment.

Greyscale levels are influenced by ultrasound system configuration,[35] which usually reflects individual operator preference. Consequently, configuration independent quantitative analysis measurements have been investigated.[13] Using image textural feature analysis, Cobo et al. predicted neonatal respiratory morbidity from foetal LUS.[36–39] Diagnostic accuracy was comparable to invasive testing requiring amniocentesis. Raimondi et al. analysed LUS images in preterm infants with respiratory distress and by combining both greyscale and textural features, the authors found a moderate correlation with oxygenation indices.[18] Similarly, Tenorio et al. reported early prediction of white matter damage using textural analysis of cranial ultrasonography.[40] In contrast, we opted for a simpler measurement, and to our knowledge, this is the first study to compare Q-LUS$_{MGV}$ with dynamic changes in lung volume. Measurement of Q-LUS$_{MGV}$ was performed with open-sourced image analysis software,[25] negating the need for purpose-built programme development. Ultrasound settings were not altered between subjects, mitigating external influence from system settings. Standardisation of ultrasound settings and incorporating advanced analysis may improve the performance of this approach and warrants consideration in future studies.

The importance of placing ventilation on the deflation limb of the PV relationship is recognised.[26,41–44] Using oxygenation as an approximation of lung volume, open lung ventilation strategies optimise lung volume by recruiting the lung to near total lung capacity using stepwise increases in continuous distending pressure, followed by gradual pressure reductions to place ventilation just above closing pressure of the lung.[30,42] This process maps the quasistatic PV relationship of the respiratory system, delineating crucial points during the inflation and deflation series. An attractive alternative is to measure anatomical recruitment using bedside LUS. However, despite proven diagnostic utility,[5,8,9,45–48] categorical LUS scoring systems[5,6] are not designed to discriminate dynamic and small changes in lung volume.[12] In contrast, Q-LUS$_{MGV}$ is a continuous measurement, which in 8-bit depth can discriminate 255 increments of greyscale, exceeding human capabilities.[17] Higher bit sampling may detect even smaller differences. In our study, Q-LUS$_{MGV}$ identified key features of the PV relationship of the respiratory system in the preterm lung. Clear inflation and deflation limbs were able to be fitted to a known model of the PV relationship.[28] Relatively small changes in lung volume were detected by significant changes in Q-LUS$_{MGV}$, particularly during the deflation series. Although this may be limited to homogenous lung disease, these findings support the hypothesis that objective measurements using image

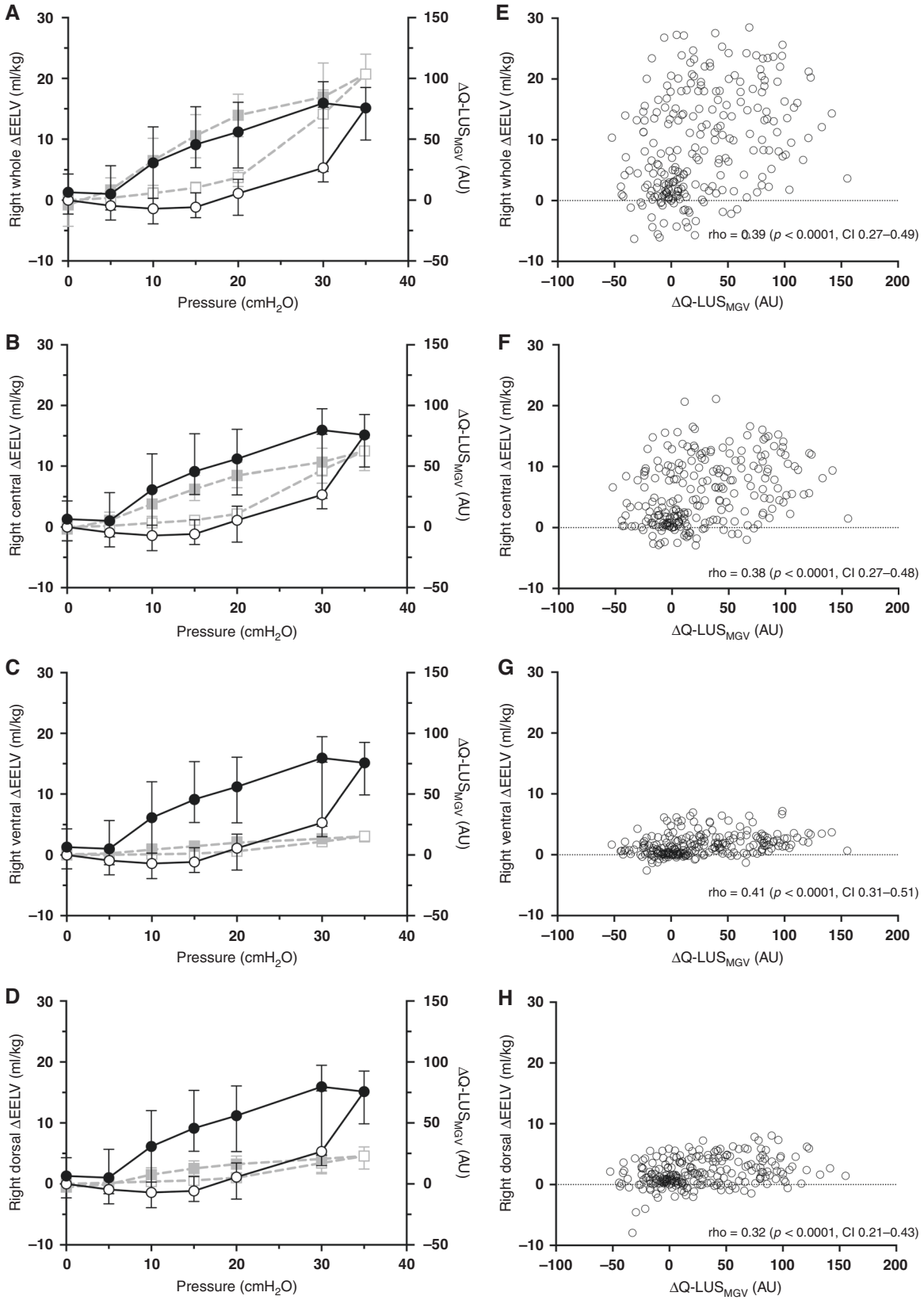


Fig. 4 Dependent lung. A–D Static regional PV curves from EIT (squares, grey dashed line) of the whole right lung (**A**), ventral (**B**), central (**C**) and dorsal (**D**) regions and Q-LUS$_{MGV}$ from dependent lung imaging (circles, black solid line). All data median (IQR). ΔQ-LUS$_{MGV}$ normalised to baseline. Open shapes represent the inflation limb and closed shapes the deflation limb. **E–H** Correlation between ΔQ-LUS$_{MGV}$ and regional lung volume for the corresponding lung regions in panels **A–D**. AU arbitrary units, CI confidence interval, cm H_2O centimetres of water, EELV end-expiratory lung volume, rho Spearman's correlation co-efficient, Q-LUS$_{MGV}$ quantitative lung ultrasound mean grey value. Left axis: lung volume (ml/kg). Right axis: ΔQ-LUS$_{MGV}$.

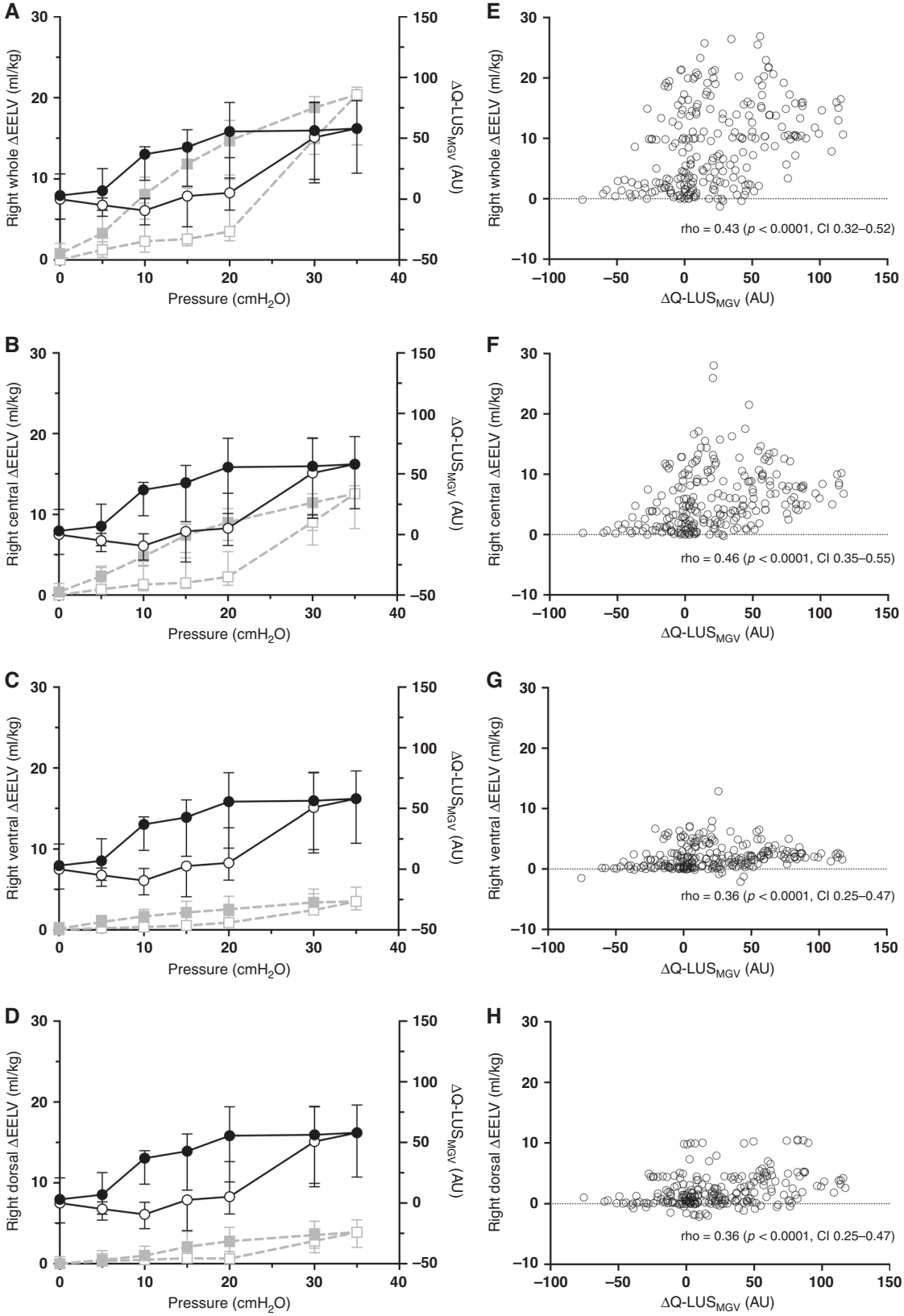


Fig. 5 Non-dependent lung. A–D Static regional PV curves from EIT (squares, grey dashed line) of the whole right lung (**A**), ventral (**B**), central (**C**) and dorsal (**D**) regions and ΔQ-LUS$_{MGV}$ from non-dependent lung imaging (circles, black solid line). All data median (IQR). ΔQ-LUS$_{MGV}$ normalised to baseline. Open shapes represent the inflation limb and closed shapes the deflation limb. **E–H** Correlation between ΔQ-LUS$_{MGV}$ and regional lung volume for the corresponding lung regions in panels **A–D**. AU arbitrary units, CI confidence interval, cm H_2O centimetres of water, EELV end-expiratory lung volume, rho Spearman's correlation co-efficient, Q-LUS$_{MGV}$ quantitative lung ultrasound mean grey value. Left axis: lung volume (ml/kg). Right axis: ΔQ-LUS$_{MGV}$.

analysis may improve the ability of LUS to detect dynamic lung volume changes in real time.

Selective LUS imaging has shown promise in early homogenous lung disease;[6,9] however, as gravity-dependent aeration distribution progresses, global imaging has increased diagnostic utility.[49,50] As lung recruitment is a continuous process, selective imaging may be more practical. It was unknown whether selective Q-LUS$_{MGV}$ correlates with changes in regional lung volume. We addressed this by comparing changes in regional lung volume derived from EIT to Q-LUS$_{MGV}$. We demonstrated a fair correlation between Q-LUS$_{MGV}$ and regional lung volumes in all areas of the lung. Despite smaller EELV being delivered to the ventral and dorsal lung, correlation was similar between regions. This was possibly due to relatively equal aeration secondary to the smaller absolute size of the dorsal and ventral regions and to homogenous lung pathology. In early respiratory distress syndrome secondary to surfactant deficiency, Q-LUS$_{MGV}$ of a single region may reflect changes in both total and regional lung volume. Further studies are required to determine whether this is true in lung conditions associated with inhomogeneous aeration.

Our study has limitations. Application of our findings to human newborns remains to be established. However, the preterm lamb is a well-established model of the preterm lung with a strong track record of translation to human research.[21] Imaging was limited to the right lung due to the rapid nature of PV relationship mapping and physical constraints. Whether whole lung Q-LUS$_{MGV}$ more precisely detects changes in lung volume warrants further investigation. Greyscale image analysis currently is not available in real time, limiting the use of this method to offline measurements and research purposes. Development of this technique to function in real time is warranted. Another limitation of this study was that lambs were subject to a brief ventilation period followed by 30 min of apnoea on placental support, leading to significant collapse and potential lung fluid accumulation. It is possible that longer ventilation off placental support may lead to more lung recruitment and a wider range of Q-LUS$_{MGV}$. Finally, although Q-LUS$_{MGV}$ significantly correlated with lung volumes, inter-subject variability was notable. Incorporation of additional feature analysis may improve the precision of this technique.

Our study has strengths. This study is the largest LUS study using the preterm lamb as a model of the preterm lung that compares LUS to gold standard, absolute and regional measurements of lung volume. The use of EIT is a novel addition, suggesting that in homogenous lung disease, changes in selected regional lung imaging are representative of changes in total lung volume. Finally, interobserver agreement between the two blinded investigators was excellent, suggesting that this measurement is reproducible between operators of varying levels of experience.

CONCLUSIONS

Greyscale image analysis using computer-assisted quantitative LUS detected real-time changes in total and regional lung volume, and reliably mapped the PV relationship in the preterm lamb. This measurement may supplement traditional LUS in discerning dynamic changes in lung volume in preterm infants at the bedside. Further work is needed to improve the precision of this technique prior to clinical translation.

DATA AVAILABILITY

Individual animal data collected during the study and statistical analysis will be available beginning 3 months and ending 23 years after article publication to researchers who provide a methodologically sound proposal with approval by an independent review committee. Data will be available for analysis to achieve the aims in the approved proposal. Proposals should be directed to arun.sett@mcri.edu.au; to gain access, data requestors will need to sign a data access or material transfer agreement approved by the Murdoch Children's Research Institute.

REFERENCES

1. De Luca, D. et al. Personalized medicine for the management of RDS in preterm neonates. *Neonatology* **118**, 127–138 (2021).
2. Thome, U., Töpfer, A., Schaller, P. & Pohlandt, F. Comparison of lung volume measurements by antero-posterior chest X-ray and the Sf6 washout technique in mechanically ventilated infants. *Pediatr. Pulmonol.* **26**, 265–272 (1998).
3. Frerichs, I. et al. Chest electrical impedance tomography examination, data analysis, terminology, clinical use and recommendations: consensus statement of the Translational EIT Development Study Group. *Thorax* **72**, 83–93 (2017).
4. Lichtenstein, D. A. & Mauriat, P. Lung ultrasound in the critically ill neonate. *Curr. Pediatr. Rev.* **8**, 217–223 (2012).
5. Brat, R. et al. Lung ultrasonography score to evaluate oxygenation and surfactant need in neonates treated with continuous positive airway pressure. *JAMA Pediatr.* **169**, e151797 (2015).
6. Raimondi, F. et al. Can neonatal lung ultrasound monitor fluid clearance and predict the need of respiratory support? *Crit. Care* **16**, R220 (2012).
7. Raimondi, F. et al. Lung ultrasound for diagnosing pneumothorax in the critically ill neonate. *J. Pediatr.* **175**, 74–78.e71 (2016).
8. Raimondi, F. et al. Lung ultrasound score progress in neonatal respiratory distress syndrome. *Pediatrics* **147**, e2020030528 (2021).
9. Badurdeen, S. et al. Lung ultrasound during newborn resuscitation predicts the need for surfactant therapy in very- and extremely preterm infants. *Resuscitation* **162**, 227–235 (2021).
10. Bouhemad, B. et al. Bedside ultrasound assessment of positive end-expiratory pressure-induced lung recruitment. *Am. J. Respir. Crit. Care Med.* **183**, 341–347 (2011).
11. Sett, A. et al. Lung ultrasound of the dependent lung detects real-time changes in lung volume in the preterm lamb. *Arch. Dis. Child. Fetal Neonatal Ed.* https://doi.org/10.1136/archdischild-2022-323900 (2022).
12. Chiumello, D. et al. Assessment of lung aeration and recruitment by CT scan and ultrasound in acute respiratory distress syndrome patients. *Crit. Care Med.* **46**, 1761–1768 (2018).
13. Mongodi, S. et al. Quantitative lung ultrasound: technical aspects and clinical applications. *Anesthesiology* **134**, 949–965 (2021).
14. Du, J., Tan, J., Yu, K. & Wang, R. Lung recruitment maneuvers using direct ultrasound guidance: a case study. *Respir. Care* **60**, e93–e96 (2015).
15. Tusman, G., Acosta, C. M. & Costantini, M. Ultrasonography for the assessment of lung recruitment maneuvers. *Crit. Ultrasound J.* **8**, 8 (2016).
16. Li, D. K., Liu, D. W., Long, Y. & Wang, X. T. Use of lung ultrasound to assess the efficacy of an alveolar recruitment maneuver in rabbits with acute respiratory distress syndrome. *J. Ultrasound Med.* **34**, 2209–2215 (2015).
17. Dambrosio, F., Amy, D. & Colombo, A. B-mode color sonographic images in obstetrics and gynecology: preliminary report. *Ultrasound Obstet. Gynecol.* **6**, 208–215 (1995).
18. Raimondi, F. et al. Visual assessment versus computer-assisted gray scale analysis in the ultrasound evaluation of neonatal respiratory status. *PLoS One* **13**, e0202397 (2018).
19. Miedema, M., de Jongh, F. H., Frerichs, I., van Veenendaal, M. B. & van Kaam, A. H. Changes in lung volume and ventilation during lung recruitment in high-frequency ventilated preterm infants with respiratory distress syndrome. *J. Pediatr.* **159**, 199–205.e192 (2011).
20. Tingay, D. G. et al. Spatiotemporal aeration and lung injury patterns are influenced by the first inflation strategy at birth. *Am. J. Respir. Cell Mol. Biol.* **54**, 263–272 (2016).
21. Tingay, D. G. et al. Gradual aeration at birth is more lung protective than a sustained inflation in preterm lambs. *Am. J. Respir. Crit. Care Med.* **200**, 608–616 (2019).
22. Tingay, D. G. et al. Imaging the respiratory transition at birth: unravelling the complexities of the first breaths of life. *Am. J. Respir. Crit. Care Med.* **204**, 82–91 (2021).
23. Victorino, J. A. et al. Imbalances in regional lung ventilation: a validation study on electrical impedance tomography. *Am. J. Respir. Crit. Care Med.* **169**, 791–800 (2004).
24. Percie du Sert, N. et al. The Arrive Guidelines 2.0: updated guidelines for reporting animal research. *PLoS Biol.* **18**, e3000410 (2020).
25. Schindelin, J. et al. Fiji: an open-source platform for biological-image analysis. *Nat. Methods* **9**, 676–682 (2012).
26. Tingay, D. G. et al. Effectiveness of individualized lung recruitment strategies at birth: an experimental study in preterm lambs. *Am. J. Physiol. Lung Cell Mol. Physiol.* **312**, L32–L41 (2017).

27. Tingay, D. G. et al. Effect of sustained inflation vs. stepwise peep strategy at birth on gas exchange and lung mechanics in preterm lambs. *Pediatr. Res.* **75**, 288–294 (2014).
28. Venegas, J. G., Harris, S. & Simon, B. A comprehensive equation for the pulmonary pressure-volume curve. *J. Appl. Physiol.* **84**, 389–395 (1998).
29. Team, R. C. R: A Language and Environment for Statistical Computing. R Foundation for Statistical Computing. (2021).
30. De Jaegere, A., van Veenendaal, M. B., Michiels, A. & van Kaam, A. H. Lung recruitment using oxygenation during open lung high-frequency ventilation in preterm infants. *Am. J. Respir. Crit. Care Med.* **174**, 639–645 (2006).
31. Tingay, D. G., Mills, J. F., Morley, C. J., Pellicano, A. & Dargaville, P. A. The deflation limb of the pressure-volume relationship in infants during high-frequency ventilation. *Am. J. Respir. Crit. Care Med.* **173**, 414–420 (2006).
32. Tingay, D. G., Mills, J. F., Morley, C. J., Pellicano, A. & Dargaville, P. A. Indicators of optimal lung volume during high-frequency oscillatory ventilation in infants. *Crit. Care Med.* **41**, 237–244 (2013).
33. Corradi, F. et al. Quantitative analysis of lung ultrasonography for the detection of community-acquired pneumonia: a pilot study. *BioMed. Res. Int.* **2015**, 1–8 (2015).
34. Corradi, F. et al. Computer-aided quantitative ultrasonography for detection of pulmonary edema in mechanically ventilated cardiac surgery patients. *Chest* **150**, 640–651 (2016).
35. Steffel, C. N. et al. Influence of ultrasound system and gain on grayscale median values. *J. Ultrasound Med.* **38**, 307–319 (2019).
36. Burgos-Artizzu, X. P., Perez-Moreno, A., Coronado-Gutierrez, D., Gratacos, E. & Palacio, M. Evaluation of an improved tool for non-invasive prediction of neonatal respiratory morbidity based on fully automated fetal lung ultrasound analysis. *Sci. Rep.* **9**, 1950 (2019).
37. Bonet-Carne, E. et al. Quantitative ultrasound texture analysis of fetal lungs to predict neonatal respiratory morbidity. *Ultrasound Obstet. Gynecol.* **45**, 427–433 (2015).
38. Palacio, M. et al. Prediction of neonatal respiratory morbidity by quantitative ultrasound lung texture analysis: a multicenter study. *Am. J. Obstet. Gynecol.* **217**, 196.e191–e196.e114 (2017).
39. Cobo, T. et al. Feasibility and reproducibility of fetal lung texture analysis by automatic quantitative ultrasound analysis and correlation with gestational age. *Fetal Diagn. Ther.* **31**, 230–236 (2012).
40. Tenorio, V. et al. Correlation between a semiautomated method based on ultrasound texture analysis and standard ultrasound diagnosis using white matter damage in preterm neonates as a model. *J. Ultrasound Med.* **30**, 1365–1377 (2011).
41. Lachmann, B. Open up the lung and keep the lung open. *Intensive Care Med.* **18**, 319–321 (1992).
42. Rimensberger, P. C., Cox, P. N., Frndova, H. & Bryan, A. C. The open lung during small tidal volume ventilation: concepts of recruitment and "optimal" positive end-expiratory pressure. *Crit. Care Med.* **27** 1946–1952 (1999).
43. van Kaam, A. H. et al. Positive pressure ventilation with the open lung concept optimizes gas exchange and reduces ventilator-induced lung injury in newborn piglets. *Pediatr. Res.* **53**, 245–253 (2003).
44. van Veenendaal, M. B., van Kaam, A. H., Haitsma, J. J., Lutter, R. & Lachmann, B. Open lung ventilation preserves the response to delayed surfactant treatment in surfactant-deficient newborn piglets. *Crit. Care Med.* **34**, 2827–2834 (2006).
45. Raimondi, F. et al. Neonatal lung ultrasound and surfactant administration: a pragmatic, multicenter study. *Chest* **160**, 2178–2186 (2021).
46. Raimondi, F. et al. Use of neonatal chest ultrasound to predict noninvasive ventilation failure. *Pediatrics* **134**, e1089–e1094 (2014).
47. Raimondi, F. et al. A multicenter lung ultrasound study on transient tachypnea of the neonate. *Neonatology* **115**, 263–268 (2019).
48. De Martino, L. et al. Lung ultrasound score predicts surfactant need in extremely preterm neonates. *Paediatrics* **142**, e20180463 (2018).
49. Pezza, L. et al. Meta-analysis of lung ultrasound scores for early prediction of bronchopulmonary dysplasia. *Ann. Am. Thorac. Soc.* **19**, 659–667 (2021).
50. Loi, B. et al. Lung ultrasound to monitor extremely preterm infants and predict bronchopulmonary dysplasia. a multicenter longitudinal cohort study. *Am. J. Respir. Crit. Care Med.* **203**, 1398–1409 (2021).

AUTHOR CONTRIBUTIONS

A.S. and D.G.T. developed the concept and designed the experiment. A.S., D.G.T., P.M.P.-F., K.R.K., R.J.S., E.J.P., J.D.C. and M.S. were involved in all lamb experimental work. A.S. and D.G.T. supervised all aspects of the study. A.S. acquired the ultrasound images. A.S. and G.F. performed the image analysis. A.S. performed the statistical analysis. A.S., G.F., P.M.P.-F., S.R.R., B.J.M., P.G.D. and D.G.T. interpreted the data. All authors participated in result interpretation. A.S. wrote the first draft and all authors contributed to redrafting the manuscript.

FUNDING

This study is supported by the Victorian Government Operational Infrastructure Support Program (Melbourne, Australia) and a grant from the National Health and Medical Research Council (NHMRC; Grant ID 1182676). A.S. is supported by a research grant from the Australasian Society of Ultrasound in Medicine, a PhD scholarship from the Centre of Research Excellence in Newborn Medicine, Melbourne and a Research Training Program PhD fee-offset scholarship from the Victorian Government. D.G.T. is supported by a Royal Children's Hospital Foundation Clinical Scientist Fellowship and NHMRC Investigator (Grant ID 2008212). P.G.D. is supported by an NHMRC Practitioner Fellowship (Grant ID 556600). B.J.M. is supported by a Medical Research Future Fund (Australia) Fellowship Grant (Grant ID 1159225). GE Healthcare provided the Logiq E ultrasound system but was not involved in the study design, analysis, or interpretation of results. Open Access funding enabled and organized by CAUL and its Member Institutions.

COMPETING INTERESTS

The authors declare no competing interests.

ETHICS APPROVAL AND CONSENT TO PARTICIPATE

The study was approved by the Murdoch Children's Research Institute Animal Ethics Committee, Melbourne, Australia (Project A923) in accordance with National Health and Medical Research Council guidelines and is reported as per the ARRIVE guidelines.

ADDITIONAL INFORMATION

Supplementary information The online version contains supplementary material available at https://doi.org/10.1038/s41390-022-02316-0.

Correspondence and requests for materials should be addressed to Arun Sett.

Reprints and permission information is available at http://www.nature.com/reprints

Publisher's note Springer Nature remains neutral with regard to jurisdictional claims in published maps and institutional affiliations.

Open Access This article is licensed under a Creative Commons Attribution 4.0 International License, which permits use, sharing, adaptation, distribution and reproduction in any medium or format, as long as you give appropriate credit to the original author(s) and the source, provide a link to the Creative Commons license, and indicate if changes were made. The images or other third party material in this article are included in the article's Creative Commons license, unless indicated otherwise in a credit line to the material. If material is not included in the article's Creative Commons license and your intended use is not permitted by statutory regulation or exceeds the permitted use, you will need to obtain permission directly from the copyright holder. To view a copy of this license, visit http://creativecommons.org/licenses/by/4.0/.

© Crown 2022